DOI: 10.1002/ejic.200700415

Synthesis and Reactivity of New Bis(tetramethylpiperidino)(phosphanyl)-alumanes

Tassilo Habereder,[a,b] Heinrich Nöth,*[a] and Robert T. Paine*[b]

Dedicated in memory of Professor Robert W. Parry

Keywords: Aminoalumanes / Phosphanylalumanes / Carbon dioxide insertion / Phosphanylcarbonate ligand / Structure elucidation

Syntheses for the new bis(2,2,6,6-tetramethylpiperidino)-(phosphanyl)alumanes, $tmp_2AlP(SiMe_3)_2$, $tmp_2AlP(SnMe_3)_2$ and $(tmp_2Al)_2PPh$ are described along with spectroscopic characterization and X-ray crystallographic structure determinations. In addition, the insertion reactions between $tmp_2AlP(SiMe_3)_2$ and CO_2, COS and CS_2 are described and compared with the outcomes for CO_2 insertion reactions with tmp_2AlCl and tmp_2AlMe. In the case of the amino-phosphanyl-alumane, the Al–P bond undergoes the insertion chemistry in contrast to Al–N bond insertions observed with tmp_2AlCl and tmp_2AlMe.

Introduction

Since the initial report on the synthesis of $(tmp_2AlH)_2$ (tmp = 2,2,6,6-tetramethyl-piperidino)[1] steady development of the chemistry of the sterically congested tmp_2Al– fragment has led to the discovery of several structurally interesting compounds that are unique in comparison to other (alkylamido)alumanes as well as (alkylamido)boranes.[2–8] In particular, the bulky tmp group shows little tendency to participate in bridge bonding and the halide compounds, tmp_2AlX [X = Cl (**1**), Br, I], are monomeric in the gas phase, in solutions and in the solid state.[2] The fluoride and hydride analogues, on the other hand, form dimers, $(tmp_2AlX)_2$ (X = F, H), through Al–F–Al and Al–H–Al bridge bonding. The halides undergo nucleophilic displacement forming a variety of tmp_2AlX (X = OR, SR, NR_2, PR_2, AsR_2, CR_3 and $Si(SiMe_3)_3$) compounds all of which are monomeric.[5] Crystallographic structure studies and computational modelling indicate that these compounds develop little or no Al–N-pp(π) bonding interactions. Instead, the Al–N bonds can be considered to possess highly polar sigma-bond character.

As part of a continuing interest in the reactivity and utility of tmp_2AlX reagents as synthons, we set out in this study to expand the available range of phosphanyl derivatives for this fragment. In the initial study mentioned above, only the formation of tmp_2AlPPh_2 was described.[5] As expected, this compound provides limited potential for use in, for example, N–Al–P ring or cage construction chemistry. In the current study, we directed attention to the synthesis of additional examples of (amino)(phosphanyl)alumanes and their reactivity.

[a] Department of Chemistry, University of Munich, Butenandtstr. 5–13, 81377, München, Germany
E-mail: H.Noeth@lrz.uni-muenchen.de
[b] Department of Chemistry, University of New Mexico, Albuquerque, NM 87131, USA
E-mail: rtpaine@unm.edu

Synthesis and Reactions

Prior work in our group with (amino)(phosphanyl)boranes[9] suggested that the molecule tmp_2AlPH_2 might be an excellent building block for the construction of novel ring and cage compounds and this compound was the initial synthetic target. Numerous attempts to accomplish the 1:1 reaction of tmp_2AlCl with $LiPH_2$·dme, as shown in Equation (1), were fruitless.

$$tmp_2AlCl + LiPH_2{\cdot}dme \xrightarrow[-LiCl]{hexane} tmp_2AlPH_2 \quad (1)$$

At 23 °C, the combination proved unreactive while under solvent reflux conditions tmpH formed along with insoluble solids some of which is LiCl. Efforts to employ Me_3Si-PH_2 directly in elimination chemistry with **1** or with strong base promotion also led to the formation of tmpH along with $(Me_3Si)_3P$ and slightly soluble, unidentified solids that may be oligomeric aminoalumane species. These results led to the subsequent studies of reactions between tmp_2AlCl and $LiP(SiMe_3)_2$·$(thf)_2$, $LiP(SnMe_3)_2$ and $LiP(H)Ph$·$(thf)_n$.

Combination of one equivalent of **1** with one equivalent of $LiP(SiMe_3)_2{\cdot}(thf)_2$ or $LiP(SnMe_3)_2$ in hexane gave the respective (amino)(phosphanyl)alumanes **2** and **3** according to Equation (2). The substitution reactions are quantitative as evidenced by NMR analysis.

$$tmp_2AlCl + LiPR_2 \xrightarrow[-LiCl]{\text{hexane}} tmp_2AlPR_2$$

2: R = $SiMe_3$

3: R = $SnMe_3$ (2)

Following recrystallization from cold hexane, the compounds are isolated as analytically pure, colorless crystalline solids in 65–70% yield. The compounds are stable indefinitely at 23 °C in the absence of moisture and oxygen.

In a similar fashion, the 1:1 combination of **1** with $LiP(H)Ph{\cdot}(thf)_n$ unexpectedly gave the (amino)(phosphanyl)alumane **4**, which likely forms in two steps summarized in Equations (3) and (4).

$$tmp_2AlCl + LiP(H)Ph \xrightarrow[-LiCl]{\text{hexane}} tmp_2AlP(H)Ph \quad (3)$$

$$tmp_2AlP(H)Ph + tmp_2AlCl \xrightarrow[-HCl]{\text{hexane}} (tmp_2Al)_2PPh$$

4 (4)

The initial combination of reagents at –78 °C produced no reaction; however, warming the mixture to 23 °C with stirring resulted in sluggish elimination of LiCl and formation, in low yield, of the anticipated product, $tmp_2AlP(H)Ph$, with a ^{31}P NMR resonance at δ = –112 ppm. Efforts to isolate this compound in pure form were not successful and attempts to complete the substitution by solvent reflux led to three additional ^{31}P NMR resonances, δ = –51, –72 and –96 ppm. The last corresponds to **4** obtained in about 45% yield in the crude reaction mixture. Following separation and recrystallization from cold hexane, **4** was isolated as colorless crystals in 33% yield. The species responsible for the ^{31}P resonances at δ = –51 and –72 ppm remain unidentified at this time.

Thwarted in our attempts to form $tmp_2Al–PH_2$ or $tmp_2Al–P(H)R$ reagents for systematic ring and/or cage construction chemistry, attention was turned to examinations of Me_3SiCl and Me_3SnCl elimination chemistry of **2** and **3** that might support ring/cage assembly processess. Such elimination chemistry routes have been used previously by us with (amino)(halo)boranes to form (amino)(phosphanyl)borane rings and cages.[9–15] In the present cases, the 1:1 combinations of BCl_3, $AlCl_3$ and $GaCl_3$ with **2** or **3** in hexane at 23 °C led to the formation of **1** identified by ^1H NMR (δ = 1.29, 1.40, 1.57) and very likely the respective $[MCl_2P(SiMe_3)_2]_n$ and $[MCl_2P(SnMe_3)_2]_n$ (M = B, Al, Ga) compounds. Attempts to obtain analytically pure samples and/or single crystals of the latter compounds were unsuccessful. These results indicate that alternative approaches will be required in the pursuit of systematic synthetic pathways for the construction of new ring and cage compounds containing multiple N–Al–P components.

Historically, another reactivity pathway of interest in our group is that involving insertion reactions into P–N,[16] B–N[17] and Al–N[18] bonds. In the current context, we have previously reported the reactions of $Al(NMe_2)_3$ and $Al(Cl)(NMe_2)_2$ with CO_2[19] and CS_2.[18] Each Al–N bond undergoes insertion with the formation of the corresponding carbamate or dithiocarbamate compounds, $Al(X_2CNMe_2)_3$ and $Al(Cl)(X_2CNMe_2)_2$ (X = O or S). A single-crystal X-ray structure determination for $Al(S_2CNMe_2)_3$ confirmed the formation of an unusual six coordinate aluminum center with bidentate dithiocarbamate chelation.[18] In close parallel to the present study, we have also previously observed CO_2 insertion in Al–N bonds in tmpAl fragments.[5,8] With the (amino)(phosphanyl)alumane, **2**, the question of interest was: will this reagent, with both Al–N and Al–P bonds, undergo selective insertion or insertion in all Al–N and Al–P bonds?

For comparison, the reaction of **1** with CO_2 was examined first. Slow diffusion of CO_2 gas into a hexane solution of **1** held first at –78 °C and then at 23 °C led over several days to the formation of a brown oil as summarized in Equation (5).

$$tmp_2AlCl + CO_2 \xrightarrow[23\ ^\circ C]{\text{hexane}} (tmp)(tmpCO_2)AlCl$$

5 (5)

The oil was extracted with hexane and concentration led to the isolation of **5** as a crystalline solid. Although excess CO_2 was present, no evidence for double insertion was obtained. However, it cannot be ruled out that such a product is present in the brown oil that resists crystallization.

The combinations of **2** with excess CO_2, COS and CS_2 led to complete conversion of **2** to the insertion products **6**–**8** as summarized in Equation (6).

$$tmp_2AlP(SiMe_3)_2 + CXX' \longrightarrow tmp_2Al\begin{matrix}X'\\ \diagup\ \diagdown\\ X\end{matrix}CP(SiMe_3)_2$$

2

6: X = X' = O

8: X = X' = S

7: X = O; X' = S (6)

The compounds **6** and **7** are obtained in high yield (90–95%) as colorless and faintly yellow crystals, respectively. Compound **8** was isolated as a red oil along with small amounts of tmpH and $(Me_3Si)_3P$. All attempts to isolate a crystalline sample of **8** for X-ray analysis failed.

NMR Characterization

The ^{1}H, $^{13}C\{^{1}H\}$, ^{31}P, ^{27}Al and ^{119}Sn NMR spectra were recorded as appropriate for **2**–**8**. The spectra for **2**–**4** can be compared with data for **1** and tmp_2AlPPh_2,[5] and the spectra for **5**–**8** can be examined against data for $[MeAl(O_2Ctmp)_2]_2$,[5] $[(tBuAl)_2(O_2Ctmp)_3]^+[tBu_3AlBrAltBu_3]^-$[8] and $Al(S_2CNMe_2)_3$.[18] In each of the new compounds **2**–**8**, the ^{1}H and $^{13}C\{^{1}H\}$ spectra are consistent with a single tmp group environment with free rotation about the Al–N bonds and rapid ring inversion. These spectra also show a single Me_3Si or Me_3Sn environment. The ^{31}P NMR spectra for **2** and **3** display high field resonances (δ = –238 and –282) significantly upfield from the value observed for tmp_2AlPPh_2 (δ =–42.9 ppm). This observation is typical of silyl- and stannylphosphanes and these shifts are similar to those in (amino)(phosphanyl)boranes reported previously.[9] The ^{31}P chemical shift for the bis-alumane **4** is downfield compared to **2** and **3**, and the shift (δ – 96) is comparable to related (phosphanyl)boranes.[9] The ^{31}P NMR shifts for **6**–**8** are successively shifted downfield from the starting material **2**: δ = –121.8 (CO_2), –57.8 (COS) and –16 (CS_2). This observation provides solid evidence that insertion of the small molecules occurs in the Al–P bond instead of the Al–N bond.

The ^{27}Al NMR spectra for **2** and **3** display a broad singlet at δ = 78 ($h_{1/2}$ = 3500 Hz) and 73 ($h_{1/2}$ = 3300 Hz) ppm, respectively. These are upfield of the reported shifts in tmp_2AlPPh_2, δ = 110 ppm, but similar to the shifts in tmp_2AlX δ = 74 ppm ($AsPh_2$), 75 (OPh) and 85 (Odipp) ppm.[5] The line widths are somewhat lower than in other tmp_2AlX compounds (ca. 8000–14,000 Hz), but in all cases they are characteristic of asymmetric, lower coordination environments on ^{27}Al. The ^{27}Al NMR spectra for the insertion products **5**–**8** are very similar. Each displays a broad single resonance in the range δ = 75–81 ppm with $h_{1/2}$ = 3400–3600 Hz. These can be compared to the ^{27}Al NMR spectrum for $[(tBuAl)_2(O_2Ctmp)_3]^+[tBu_3AlBrAltBu_3]^-$ that shows a single broad resonance for the Al in the cation at δ = 53 ppm ($h_{1/2}$ = 3500 Hz). As discussed in the next section, this cation contains two four coordinate *t*BuAl units bridged by three carbamate ligands.[8]

Crystal Structure Analyses

Single crystal X-ray diffraction structure determinations were completed for **2**–**7**. As found for **1**[2] and tmp_2AlPPh_2,[5] the compounds **2**–**4** are monomeric in the solid state and views of the molecules are shown in Figures 1, 2, and 3. In **2** and **3**, the tri-coordinate Al atom and tmp N atoms are planar while the phosphorus atom is pyramidal (sum of angles: **2**, 335.5°; **3**, 326.3°). The same atom geometries exist in tmp_2AlPPh_2 although the sum of angles at the P atom (316.2°) is smaller in tmp_2AlPPh_2. The Al–P bond lengths [**2**, 2.361(2) Å; **3**, 2.334(2) Å] are slightly shorter than that found in tmp_2AlPPh_2 [2.377(1) Å] but slightly longer than that reported for $trip_2Al$–P(Ada)($SiPh_3$) [2.342(2) Å] (trip = 2, 4, 6-*i*$Pr_3C_6H_2$; Ada = adamantyl).[20] The Al–N bond lengths [**2**, 1.846(4) Å and 1.848(4) Å; **3**, 1.832(4) Å and 1.818(4) Å] are slightly longer or identical to the distances in tmp_2AlPPh_2 [1.819(2) Å], while the Al–N distances in **1** are 1.785(4) Å and 1.810(4) Å.[2] These parameters are consistent with sigma-only Al–P bonding and highly polar sigma-only Al–N bonding. The molecular structure of **4** is similar (planar N and Al atom environments) to **2** and **3**, but different in that the P atom is also flat with C(37)–P(1)–Al(1) 109.1(2)°, C(37)–P(1)–Al(2) 109.4(2)° and Al(1)–P(1)–Al(2) 141.4(1)° (sum = 359.9°). The Al–P bond lengths [Al(1)–P(1), 2.287(3) Å; Al(2)–P(1), 2.292(3) Å] are slightly shorter than in **2**, **3** and tmp_2AlPPh_2 while the Al–N bond lengths [Al(1)–N(1) 1.826(5) Å, Al(1)–N(2) 1.825(5) Å, Al(2)–N(3) 1.819(5) Å, Al(2)–N(4) 1.812(5) Å] are comparable to those in **2**, **3** and tmp_2AlPPh_2. The flattened P atom environment is probably a result of steric constraints imposed by the tmp and phenyl substituent groups rather than the operation of Al–P pp–π bonding contributions. Furthermore, the N–Al–N angles in all three compounds fall in a narrow range, 121.8–132.4°, observed in other tmp_2AlX compounds: 126.6(2)° for **2**, 127.2(2)° for **3**, and 126.8(2)° for **4**.[5] These parameters are consistent with the observation that N–Al–N bond angles offer a gauge of Al–N bond polarity and large angles (> 122°) appear in compounds containing weakly basic substituents X and highly polar Al–N bonds.[5]

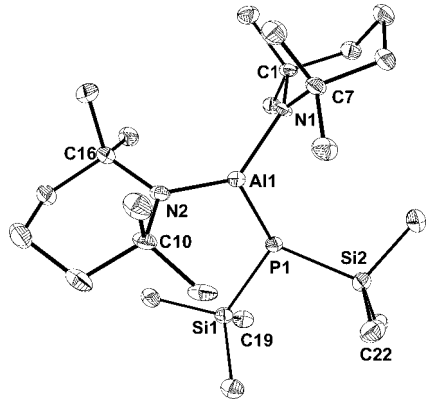

Figure 1. Molecular structure of **2**.

The core molecular structure for **5**, isolated from the reaction of **1** with CO_2, is shown in Figure 4 (tmp carbon atoms omitted for clarity). It is immediately apparent that **5** is dimeric. Furthermore, the structure reveals that CO_2 insertion takes place in only one of the two Al–N bonds and that the resulting carbamate acts as a bridging ligand toward a second Al(Cl)(tmp)(μ-O_2Ctmp) fragment. The resulting puckered eight-membered $[–Al–O–C–O–]_2$ ring has four coordinate Al atom environments with the terminal tmp groups and terminal Cl atoms in *cis* orientations across the ring. The terminal Al–Cl bond lengths [Al(1)–Cl(1) 2.164(2) Å and Al(2)–Cl(2) 2.159(1) Å] are slightly longer than the Al–Cl bond lengths in tmp_2AlCl, [2.144(2) Å] and in $(Me_2NAlCl_2)_2$ [2.088(3) Å and 2.123(3) Å].[21] The terminal Al–N bond lengths [Al(1)–N(2) 1.805(3) Å and Al(2)–N(4) 1.826(3) Å can be compared with the values in

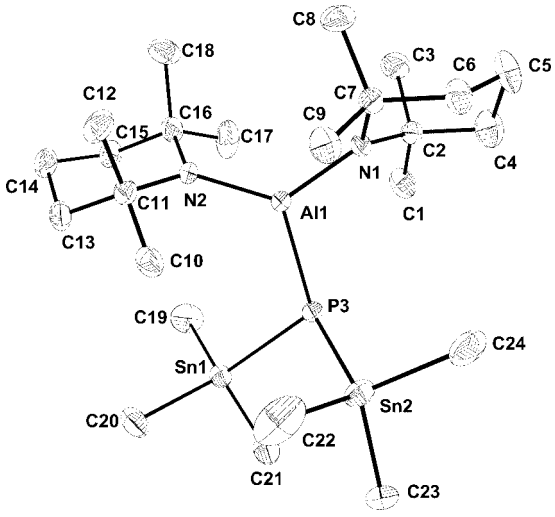

Figure 2. Molecular structure of **3**.

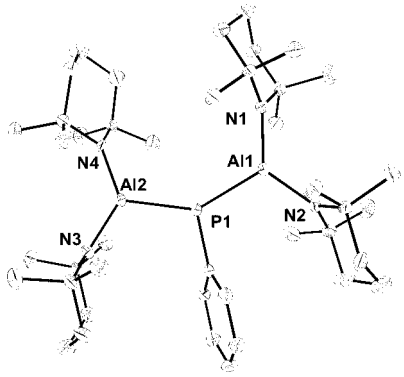

Figure 3. Molecular structure of **4**.

tmp_2AlCl [1.785(4) and 1.810(4) Å]. The bonding parameters in the carbamate ligands are fairly symmetrical with N(1)–C(2) 1.328(4) Å, N(3)–C(1) 1.330(5) Å, O(1)–C(2) 1.289(4) Å O(4)–C(2) 1.275(4) Å, O(2)–C(1) 1.289(4) Å and O(3)–C(1) 1.271(4) Å. The carbamate bridging interactions with the two Al atoms are also relatively symmetrical with Al–O (avg) = 1.78(1) Å [Al(1)–O(1) 1.784(3) Å, Al(1)–O(2) 1.789(3) Å, Al(2)–O(3) 1.776(3) Å, Al(2)–O(4) 1.790(2) Å]. These Al–O bond lengths are significantly shorter than in the related but more fragile complex $[MeAl(O_2Ctmp)_2]_2$ whose four bridging bidentate carbamate ligands form a paddle-wheel structure with Al–O bond lengths in a range 1.863(3) to 1.880(3) Å.[5] On the other hand, the bonding parameters in **5** are similar to those in the cation $[(t\text{BuAl})_2(O_2Ctmp)_3]^+$: Al–O (avg) 1.763(4) Å, C–O (avg) 1.292(7) Å and C–N (avg) 1.308(6) Å.[8]

In direct contrast with **5**, the molecular structure determinations for **6** and **7** reveal that insertions of CO_2 and COS take place exclusively into the Al–P bond of **2** and the resulting compounds are monomeric in the solid state as shown in Figure 5 and Figure 6. The formal phosphanylcarbonate $(Me_3Si)_2PCO_2^{1-}$ and phosphanylthiocarbonate $(Me_3Si)_2PCOS^{1-}$ units are planar and they act as bidentate

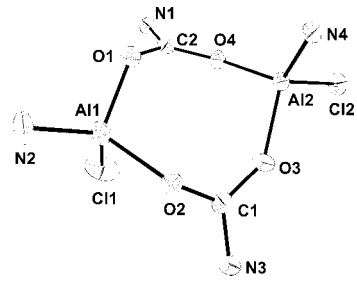

Figure 4. Molecular structure of **5** with tmp carbon atoms omitted for clarity.

chelating ligands toward tetrahedral Al centers in a formal tmp_2Al cation. The Al–N bond lengths and internal N–Al–N bond angles in the two compounds are similar: **6**, Al(1)–N(1) 1.800(6) Å, Al(1)–N(2) 1.815(6) Å and N(1)–Al(1)–N(2) 129.8(3)°; **7**, Al(1)–N(1) 1.827(5) Å, Al(1)–N(2) 1.801(5) Å, and 128.2(2)°. In both compounds the N–Al–N angle is only slightly enlarged compared with the starting compound **2**. The phosphanylcarbonate, $(Me_3Si)_2PCO_2^{1-}$, unit is symmetrically bonded to the Al center in **6**: Al(1)–O(1) 1.921(5) Å, Al(1)–O(2) 1.918(4) Å, C(1)–O(1) 1.281(7) Å, C(1)–O(2) 1.285(7) Å and C(16)–P(1) 1.814(7) Å, with internal chelate ring angles O(1)–Al(1)–O(2) 68.4(2)°, Al(1)–O(1)–C(16) 88.1(4)°, Al(1)–O(2)–C(16) 88.2(4)° and O(1)–C(16)–O(2) 114.3(6)°. The $(Me_3Si)_2PCOS^{1-}$ unit of course forms a more asymmetric chelate ring in **7**: Al(1)–O(1) 1.887(3) Å, Al(1)–S(2) 2.422(2) Å, C(1)–O(1) 1.291(6) Å, C(1)–S(2) 1.708(5) Å and C(1)–P(1) 1.796(6) Å, with internal chelate ring angles O(1)–Al–S(2) 70.9(1)°, Al–O(1)–C(1) 101.6(3)°, Al–S(2)–C(1) 71.9(2)° and O(1)–C(1)–S(2) 114.8(4)°. It is notable that the Al–O bond lengths in **6** and **7** are significantly longer than in **5** [Al–O avg 1.78(1) Å] and in the cation $[(t\text{BuAl})_2(O_2Ctmp)_3]^+$ [Al–O (avg.) 1.763(7) Å]. The Al–O distances in **6** are, in fact, even significantly longer than the Al–O (avg.) in $[MeAl(O_2Ctmp)_3]_2$. Given these bonding parameters it is a little surprising that the complex is as stable as it appears to be where the carbonate ligands are bridging two Al atoms. It is also observed that the Al–S bond length in **7** is longer than the corresponding bond length in $Al(S_2CNMe_2)_3$ [Al–S avg 2.396(1) Å].[18]

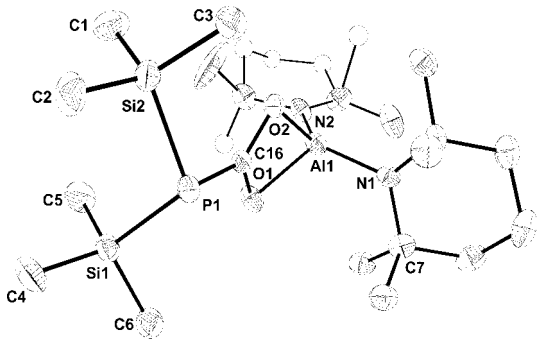

Figure 5. Molecular structure of **6**.

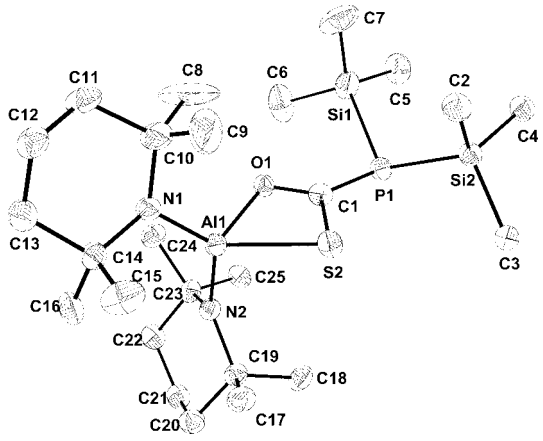

Figure 6. Molecular structure of **7**.

Conclusions

The nucleophilic substitution chemistry on tmp_2AlCl described in part in a previous report,[5] has been extended further in the present study. The initial intent was to prepare (amino)(phosphanyl)alumanes, tmp_2AlPR_2, that might find use for the construction of Al–P cage compounds related to those discovered in our prior work with (amino)-(phosphanyl)boranes.[9] Unfortunately, the principle target compound, tmp_2AlPH_2, either does not form or is unstable under forcing reaction conditions. However, three new (amino)(phosphanyl)alumanes, tmp_2AlPR_2, R = $SiMe_3$ (**2**), $SnMe_3$ (**3**) and $(tmp_2Al)_2PPh$ (**4**) were obtained and characterized.

It had been previously noted that the polar Al–N bond in (amino)alumanes is susceptible to CO_2 bond insertion.[5,8,19] In particular, both Al–N bonds in tmp_2AlCH_3 have been observed to undergo CO_2 insertion with formation of $[MeAl(tmpCO_2)_2]_2$ in which the two Al atoms are bridged by four carbamate ligands.[5] In the present study, it was expected that similar Al–N bond insertion would occur in both tmp–Al bonds of tmp_2AlCl, **1**. However, under the conditions explored, only one tmp–Al bond undergoes CO_2 insertion with resulting formation of $[Al(Cl)(tmp)(tmpCO_2)]_2$ **5**, a dimer with *two* bridging carbamate ligands and two terminal tmp groups. In a sense, this can be considered an intermediate product on the way to the formation of the compound $[MeAl(tmpCO_2)]_2$ that utilizes four bridging carbamate ligands to form a dimeric structure. Perhaps the electronic difference between Me and Cl is responsible for shutting down the reactivity of the second Al–N bond in **1**. It is also worth reviewing that $[MeAl(tmpCO_2)]_2$ is thermally unstable above –10 °C,[5] so perhaps the full insertion product from **1** is simply too unstable to allow isolation.

Molecule **2** presents the additional option that insertion might occur in the Al–P bond as well as the Al–N bonds. However, under the conditions utilized, reactions of **2** with CO_2, COS and CS_2 result *only* in Al–P bond insertion. Furthermore, crystal structure analyses indicate that the resulting phosphanylcarbonate $(Me_3Si)_2PCO_2^-$ and phosphanylthiocarbonate $(Me_3Si)_2PCOS^-$ fragments act as terminal, bidentate chelating ligands toward aluminum. Spectroscopic data, suggest that the same coordination condition results with CS_2 insertion that produces only $tmp_2Al[S_2CP(SiMe_3)_2]$.

Experimental Section

Standard inert-atmosphere techniques were used for the manipulation of all reagents and solvents were rigorously dried and distilled before use. NMR spectra were recorded on Bruker WP-250 and JEOL GSX-400 NMR spectrometers from samples flame sealed in evacuated NMR tubes containing appropriate lock solvents. Spectra were referenced with external Me_4Si (^1H and ^{13}C), 85% H_3PO_4 (^{31}P), 1 M aqueous LiCl (^7Li), 1 M aqueous $HAlCl_4$ (^{27}Al) and Me_4Sn (^{119}Sn). Downfield shifts relative to the reference were assigned positive δ values. CHN-Analytical data obtained for these compounds are low in comparison to the calculated values and this is consistent with incomplete combustion and formation of aluminum carbide or silicide residues.[22–24] X-ray diffraction: Siemens P4 four-circle diffractometer with a CCD area detector and LT2 device, Mo-K_α radiation, graphite monochromator.

Bis(trimethylsilyl)phosphanyl-bis(2,2,6,6-tetramethylpiperidino)alumane (2): A suspension of $LiP(SiMe_3)_2\cdot(thf)_2$[25] (1.3 g, 4.3 mmol) in hexane (50 mL) was slowly treated (–78 °C) with tmp_2AlCl (**1**) (1.5 g, 4.3 mmol) in hexane (50 mL). The mixture was warmed slowly with stirring and then held at 23 °C (1 h). Volatile components were vacuum-evaporated, the solid residue treated with fresh hexane (50 mL) and filtered. The filtrate was concentrated to ca. 10 mL and cooled (–78 °C). After several days colorless crystals were collected. Yield: 1.34 g (66%) of **2**, m.p. 87 °C (dec.). ^1H NMR (C_6D_6): δ = 0.46 [d, J_{HP} = 4.8 Hz, 18 H, $Si(CH_3)_3$], 1.39 [m, 8 H, CCH_2], 1.55 [s, 24 H, CCH_3], 1.62 [m, 4 H, CCH_2CH_2] ppm. $^{13}C\{^1H\}$ NMR (C_6D_6): δ = 5.5 [d, J_{CP} = 11.4 Hz, $SiCH_3$], 18.6 [CCH_2CH_2], 34.5 [CH_3], 40.7 [CCH_2], 52.7 [$C(CH_3)_2$] ppm. ^{27}Al NMR: δ = 78 ($h_{1/2}$ = 3500 Hz) ppm. $^{31}P\{^1H\}$ NMR: δ = –238 ppm. $C_{24}H_{54}AlN_2PSi_2$ (484.83): calcd. C 59.64, H 11.23, N 5.78; found C 57.70, H 9.42, N 6.80.

Bis(trimethylstannyl)phosphanyl-bis(2,2,6,6-tetramethylpiperidino)-alumane (3): A solution of $(Me_3Sn)_3P$[26] (2.91 g, 5.6 mmol) in THF (30 mL) was cooled (–78 °C) and *n*BuLi solution (3.5 mL, 5.6 mmol) in hexane was added with stirring. The mixture was warmed to 23 °C, stirred (1 h) and volatiles vacuum evaporated. The residue was treated with hexane (30 mL) and this suspension was cooled (–78 °C) and combined with tmp_2AlCl (1.9 g, 5.5 mmol) in hexane (30 mL). The mixture was warmed to 23 °C and stirred (1 h). Volatile components were removed from the resulting mixture, the residue treated with hexane (50 mL) and filtered. The filtrate was concentrated (5 mL) and cooled (–20 °C). After several days, colorless crystals deposited. Yield: 1.84 g, 69% of **3**, m.p. 103–104 °C. ^1H NMR (C_6D_6): δ = 0.46 [m, J_{HP} = 4.8, J_{HSn} = 52 Hz, 18 H, $Sn(CH_3)$], 1.36 [m, 8 H, CCH_2], 1.52 [s, 24 H, CCH_3], 1.63 [m, 4 H, CCH_2CH_2] ppm. $^{13}C\{^1H\}$ NMR (C_6D_6): δ = –3.0 [m, J_{CP} = 6.6, J_{CSn} = 295 Hz, $SnCH_3$], 18.5 [CCH_2CH_2], 34.7 [CH_3], 41.0 [CCH_2], 52.6 [$C(CH_3)_2$] ppm. ^{27}Al NMR: δ = 73 [$h_{1/2}$ = 3300 Hz] ppm. $^{31}P\{^1H\}$ NMR: δ = –282 [m, J_{PSn} = 754, 785 Hz] ppm. ^{119}Sn NMR: δ = 18.0 [d, J_{SnP} = 785 Hz] ppm. $C_{24}H_{54}AlN_2PSn_2$ (666.04): calcd. C 43.28, H 8.17, N 4.21; found C 42.65, H 8.13, N 4.02.

Phenyl-bis[bis(2,2,6,6-tetramethylpiperidino)alumanyl]phosphane (4): A solution of $PhPH_2$ (0.55 g, 4.95 mmol) in THF (30 mL) was

cooled to –78 °C and combined with *n*BuLi/hexane solution (5.0 mmol). The mixture was stirred, warmed to 23 °C and stirred further (2 h) leaving an orange suspension. The volatiles were vacuum evaporated and the solid residue suspended in hexane (30 mL). The mixture was cooled (–78 °C) and combined with tmp_2AlCl (1.7 g, 5.0 mmol) and then warmed, stirred (2 h) at 23 °C and then refluxed (2 d). The crude reaction mixture displayed ^{31}P NMR resonances at δ = –51, –72, –96 (broad) and –112. The mixture was filtered, the filtrate concentrated and cooled (–20 °C) and colorless crystals deposited which were collected and washed with cold hexane. Yield: 0.66 g, 33% of **4**, m.p. 200 °C (dec.). ^1H NMR (C_6D_6): δ = 1.25 (m, 24 H, $C(CH_2)_2$ and CCH_2CH_2), 1.61 (s, 48 H, CCH_3), 7.15 (m, 3 H Ph), 7.81 (t, J_{HH} = 6.8 Hz, 2 H, Ph) ppm. $^{31}P\{^1H\}$ NMR: δ = –96 ppm. $C_{42}H_{77}Al_2N_4P$ (722.55): calcd. C 69.77, H 10.73, N 7.75; found C 66.40, H 9.93, N 6.48.

Reaction of 1 with CO_2: Carbon dioxide gas was allowed to slowly diffuse into a sample of **1** (0.5 g, 1.5 mmol) in hexane (10 mL) held at –78 °C. The resulting mixture was allowed to stand for several days and a brownish oil formed. The oil was crystallized from a minimum of hexane at 23 °C over several weeks and a few colorless crystals of **5** were isolated. The oil was examined by NMR spectroscopy. ^1H NMR (C_6D_6): δ = 1.23, 1.46, 1.52, 1.61 ppm. ^{27}Al NMR: δ = 81 ppm.

Reaction of 2 with CO_2: A sample of **2** (1.88 g, 4.0 mmol) in hexane (5 mL) was layered over dry-ice and allowed to stand at 23 °C for several days. Orange crystals deposited. Yield: 2.0 g, 95% of **6**, m.p. 109 °C (dec.). ^1H NMR (C_6D_6): δ = 0.46 [d, J_{HP} = 5.5 Hz, 18 H, $SiCH_3$], 1.39 [m, 8 H, CCH_2], 1.51 [s, 24 H, CCH_3], 1.62 [m, 4 H, CCH_2CH_2] ppm. $^{13}C\{^1H\}$ NMR (C_6D_6): δ = 1.6 [d, J_{CP} = 12.5 Hz, $SiCH_3$], 18.7 [CCH_2CH_2], 34.3 [CH_3], 41.5 [CCH_2], 52.3 [$C(CH_3)_2$] ppm. ^{27}Al NMR: δ = 75 [$h_{1/2}$ = 3500 Hz] ppm. $^{31}P\{^1H\}$ NMR: δ = –121.8 ppm. $C_{25}H_{54}AlN_2O_2PSi_2$ (528.84): calcd. C 56.78, H 10.29, N 5.30; found C 54.59, H 9.89, N 4.78.

Reaction of 2 with COS: A sample of **2** (1.0 g, 2.1 mmol) in hexane (40 mL) was frozen at –196 °C and COS gas (2.1 mmol) was measured volumetrically and condensed on the mixture. The combined mixture was warmed to –78 °C, stirred (2 h) and then warmed to 23 °C and stirred (12 h). The resulting cloudy orange solution was filtered and the filtrate concentrated (20 mL) and cooled (–20 °C). After several days, yellow crystals deposited. Yield: 0.95 g, 95% of **7**, m.p. 111–114 °C. ^1H NMR (C_6D_6): δ = 0.37 [d, J_{HP} = 5.0 Hz, 18 H, $SiCH_3$], 1.46 [m, 8 H, CCH_2], 1.58 [s, 24 H, CCH_3], 1.67 [m, 4 H, CCH_2CH_2] ppm. $^{13}C\{^1H\}$ NMR (C_6D_6): δ = 1.7 [d, J_{CP} = 12.1 Hz, $SiCH_3$], 18.6 [CCH_2CH_2], 34.5 [CH_3], 41.7 [CCH_2], 52.9 [$C(CH_3)_2$] ppm. ^{27}Al NMR: δ = 81 ppm [$h_{1/2}$ = 3400 Hz]. $^{31}P\{^1H\}$ NMR: δ = –57.8 ppm. $C_{25}H_{54}AlN_2OPSSi_2$ (544.90): calcd. C 55.64, H 9.99, N 5.14; found C 54.90, H 9.92, N 4.74.

Reaction of 2 with CS_2: A sample of **2** (0.85 g, 1.75 mmol) in hexane (20 mL) was treated with CS_2 (0.15 mL, 1.75 mmol). The reaction mixture was stirred at 23 °C and monitored by ^{31}P NMR spectroscopy. After 36 h, no resonance due to **2** was detected. The mixture was filtered leaving a bright red solution that was concentrated (10 mL) and cooled (–78 °C). A red oil, **8**, deposited. Efforts to purify **8** by crystallization were unsuccessful. The crude product contained small amounts of $P(SiMe_3)_3$ and tmpH that were not completely removed. ^1H NMR (C_6D_6): δ = 0.40 [d, J_{HP} = 5.4 Hz, 9 H, $SiCH_3$], 0.50 [d, J_{HP} = 4.8 Hz, 9 H, $SiCH_3$], 1.2–1.5 [m, 12 H, CCH_2CH_2], 1.54 [s, 12 H, CCH_3], 1.63 [s, 12 H, CCH_3] ppm. $^{13}C\{^1H\}$ NMR (C_6D_6): δ = 1.8 [d, J_{CP} = 11.7 Hz, $SiCH_3$], 5.6 [d, J_{CP} = 11.4 Hz, $SiCH_3$], 18.4 [CCH_2CH_2], 18.6 [CCH_2CH_2], 34.5

Table 1. Crystallographic data for **2**–**5**.

	2	**3**	**4**	**5**
Code	Habe41	Habe51	Habe45	Habe55a
Formula	$C_{24}H_{54}AlN_2PSi_2$	$C_{24}H_{54}AlN_2PSn$	$C_{42}H_{77}Al_2N_4P$	$C_{38}H_{72}AlCl_2N_4O_4$
Formula weight	484.82	666.02	723.01	773.86
Crystal size [mm]	0.2 × 0.2 × 0.1	0.2 × 0.1 × 0.1	0.1 × 0.1 × 0.05	0.2 × 0.1 × 0.1
Crystal system	monoclinic	monoclinic	monoclinic	monoclinic
Space group	$P2_1/c$	$P2_1/n$	$P2_1/n$	$P2_1/c$
a [Å]	12.65(1)	12.1899(8)	17.46(3)	21.822(9)
b [Å]	11.95(1)	18.734(1)	11.14(1)	11.358(4)
c [Å]	21.46(2)	13.813(1)	22.67(3)	36.27(1)
α [°]	90	90	90	90
β [°]	105.68(2)	93.729(2)	101.65(2)	106.814(6)
γ [°]	90	90	90	90
V [Å^3]	3127(5)	3147.9(4)	4318(10)	8604(6)
Z	4	4	4	8
$P_{calcd.}$ [g cm^{-3}]	1.030	1.405	1.112	1.195
μ [mm^{-1}]	0.206	1.678	0.137	0.233
F(000)	1072	1360	1592	3360
Index range	$-13 \le h < 13$	$-16 \le h \le 16$	$-18 \le h \le 18$	$-28 \le h \le 28$
	$-12 \le k \le 12$	$-23 \le k \le 23$	$-11 \le k \le 11$	$-15 \le k \le 15$
	$-20 \le l \le 20$	$-17 \le l \le 17$	$-23 \le l < 23$	$-45 \le l \le 45$
2θ [°]	3.34–44.92	3.66–58.72	3.28–43.92	1.94–58.74
T [K]	193	193	193	193
Reflections collected	12060	18257	16616	48953
Reflections unique	3630	5561	5201	17483
Reflections observed (4σ)	2190	3920	2354	9550
R_{int}	0.0988	0.0459	0.2064	0.0703
No. of variables	285	285	458	933
GooF	0.927	1.019	0.969	1.029
Final R (4σ)	0.0525	0.0396	0.0760	0.0729
Final wR_2	0.1046	0.0864	0.1092	0.1723
Largest residual peak [e/Å^3]	0.214	0.811	0.262	0.715

Table 2. Crystallographic data for **6**, **7** and **9**.

	6	**7**	**9**
Code	Habe39	Habe42	Habe54
Formula	$C_{31}H_{126}AlN_2O_2PSi_2$	$C_{25}H_{54}AlN_2OPSSi_2$	$C_{14}H_{34}LiO_2PSn_2$
Formula weight	673.47	544.89	509.70
Crystal size [mm]	$0.3\times0.2\times0.2$	$0.2\times0.2\times0.1$	$0.2\times0.1\times0.1$
Crystal system	orthorhombic	triclinic	monoclinic
Space group	*P*2(1)2(1)2(1)	*P*1	*C*2/*c*
a [Å]	11.533(1)	8.9907(8)	18.441(3)
b [Å]	12.140(1)	12.327(1)	13.746(2)
c [Å]	23.126(1)	16.489(1)	19.074(3)
α [°]	90	103.251(1)	90
β [°]	90	96.195(2)	107.519(2)
γ [°]	90	109.0290(10)	90
V [Å^3]	3237.8(6)	1634.0(2)	4610.6(11)
Z	4	2	8
$P_{calcd.}$ [g cm^{-3}]	1.382	1.107	1.469
μ [mm^{-1}]	0.222	0.267	2.235
F(000)	1592	596	2016
Index range	$-12\le h\le12$	$-9\le h\le9$	$-23\le h\le23$
	$-13\le k\le13$	$-12\le k\le12$	$-16\le k\le16$
	$-25\le l\le25$	$-17\le l\le15$	$-24\le l\le24$
2*θ* [°]	3.52–46.50	3.66–43.94	3.76–58.24
T [K]	193	193	193
Reflections collected	14537	6490	12874
Reflections unique	4606	3316	4548
Reflections observed (4σ)	2211	2385	2726
R_{int}	0.1340	0.0287	0.0298
No. of variables	310	313	187
GooF	0.876	1.091	1.024
Final *R* (4σ)	0.0679	0.0650	0.0483
Final wR_2	0.1191	0.1755	0.1165
Largest residual peak [e/Å^3]	0.295	0.558	1.215

[C*C*H$_3$], 34.8 [C*C*H$_3$], 40.7 [C*C*H$_2$], 41.5 [C*C*H$_2$], 52.7 [*C*(CH$_3$)$_2$], 53.6 [*C*(CH$_3$)$_2$] ppm. ^{27}Al NMR: δ = 75 ppm [$h_{1/2}$ = 3600 Hz]. ^{31}P{^{1}H} NMR: δ = –16 ppm.

X-Ray Structure Determinations: Single crystals were covered with a polyfluoro ether oil and specimens mounted on the tip of glass fibers. After cooling the crystals on the goniometer head to –80 °C with the LT2 device, the unit cells were determined from reflections collected on 65 frames at five different settings of the ω and χ circles. Data collections were performed in the hemisphere mode (1200 frames) with programs implemented in SMART.[27] The program SAINT[28] was used for data reduction and absorption corrections were applied using SADABS.[29] The structures were solved by direct methods using SHELX97[30] and refined with the same package. Non-hydrogen atoms were refined with anisotropic thermal factors. Most hydrogen atoms were visible following anisotropic refinement but were placed in calculated positions and included in refinements by applying the riding model. Data related to the crystallography are summarized in Table 1 and Table 2.

CCDC-640019 to –640025 contain the supplementary crystallographic data for this paper. These data can be obtained free of charge from The Cambridge Crystallographic Data Centre via www.ccdc.cam.ac.uk/data_request/cif.

Acknowledgments

We thank the National Science Foundation (CHE-9983205) and the Fonds der Chemischen Industrie for support of this research. We also thank M. Suter for X-ray data collection on one of the compounds.

[1] C. Klein, H. Nöth, M. Tacke, M. Thomann, *Angew. Chem.* **1993**, *105*, 923–925; *Angew. Chem. Int. Ed. Engl.* **1993**, *32*, 886–888.
[2] I. Krossing, H. Nöth, C. Tacke, M. Schmidt, H. Schwenk-Kircher, *Chem. Ber./Recueil* **1997**, *130*, 1047–1052.
[3] B. N. Anand, I. Krossing, H. Nöth, *Inorg. Chem.* **1997**, *36*, 1979–1981.
[4] I. Krossing, H. Nöth, H. Schwenk-Kircher, *Eur. J. Inorg. Chem.* **1998**, 927–939.
[5] K. Knabel, I. Krossing, H. Nöth, H. Schwenk-Kircher, M. Schmidt-Amelunxen, T. Seifert, *Eur. J. Inorg. Chem.* **1998**, 1095–1114.
[6] I. Krossing, H. Nöth, H. Schwenk-Kircher, T. Seifert, C. Tacke, *Eur. J. Inorg. Chem.* **1998**, 1925–1930.
[7] K. Knabel, H. Nöth, *Z. Naturforsch., Teil B* **2005**, *60*, 155–163.
[8] K. Knabel, H. Nöth, *Z. Naturforsch., Teil B* **2005**, *60*, 1027–1035.
[9] H. Nöth, R. T. Paine, *Chem. Rev.* **1995**, *95*, 343–379.
[10] G. L. Wood, D. Dou, C. K. Narula, E. N. Duesler, R. T. Paine, H. Nöth, *Chem. Ber.* **1990**, *123*, 1455–1459.
[11] G. L. Wood, C. K. Narula, E. N. Duesler, R. T. Paine, H. Nöth, *J. Chem. Soc. Chem. Commun.* **1987**, 496–498.
[12] H. Nöth, W. Schrägle, *Z. Naturforsch., Teil B* **1961**, *16*, 473–474.
[13] H. Nöth, W. Schrägle, *Chem. Ber.* **1965**, *98*, 352–362.
[14] M. S. Lube, R. L. Wells, P. S. White, *Inorg. Chem.* **1996**, *35*, 5007–5014.
[15] R. T. Paine, H. Nöth, T. Habereder, J. F. Janik, E. N. Duesler, D. Dreissig, *ACS Symp. Ser.* **2006**, *917*, 152–165.
[16] R. W. Light, L. D. Hutchins, R. T. Paine, C. F. Campana, *Inorg. Chem.* **1980**, *19*, 3597–3604.
[17] H. Nöth, P. Schweitzer, *Chem. Ber.* **1969**, *102*, 161–166.

[18] H. Nöth, P. Konrad, *Chem. Ber.* **1983**, *116*, 3552–3558.
[19] P. Konrad, Dissertation, Univ. Marburg, **1968**.
[20] R. J. Wehmschulte, K. Ruhlandt-Senge, P. P. Power, *Inorg. Chem.* **1994**, *33*, 3205–3207.
[21] A. Ahmed, W. Schwarz, H. Hess, *Acta Crystallogr., Sect. B* **1977**, *33*, 3574–3576.
[22] J. F. Janik, E. N. Duesler, R. T. Paine, *J. Organomet. Chem.* **1997**, *539*, 19–25.
[23] J. F. Janik, E. N. Duesler, R. T. Paine, *Chem. Ber.* **1993**, *126*, 2649–2651.
[24] J. F. Janik, E. N. Duesler, W. F. McNamara, M. Westerhausen, R. T. Paine, *Organometallics* **1989**, *8*, 506–514.
[25] G. Fritz, W. Hölderich, *Z. Anorg. Allgem. Chem.* **1976**, *422*, 1104–1114.
[26] J. P. von Linthoudt, E. V. von den Berghe, G. P. von der Kelen, *Spectrochim. Acta, Part A* **1980**, *36*, 17–21.
[27] *SMART*, Bruker Analytical Instruments, Madison, version 5.1.
[28] *SAINT*, Bruker Analytical Instruments, Madison, version 5.1.
[29] *SADABS*, Absorption corrections as implemented in *SHELXTL*, Bruker Analytical Instruments, Madison, version 5.1.
[30] *SHELXTL*, Bruker Analytical Instruments, Madison, version 5.1.

Received: April 16, 2007
Published Online: July 18, 2007

